The Astrophysical Journal, 684: L95–L98, 2008 September 10

FIRST RESOLVED IMAGES OF THE ECLIPSING AND INTERACTING BINARY β LYRAE

M. Zhao,[1] D. Gies,[2] J. D. Monnier,[1] N. Thureau,[3] E. Pedretti,[3] F. Baron,[4] A. Merand,[2] T. ten Brummelaar,[2] H. McAlister,[2] S. T. Ridgway,[5] N. Turner,[2] J. Sturmann,[2] L. Sturmann, [2] C. Farrington,[2] and P. J. Goldfinger[2]

Received 2008 May 5; accepted 2008 July 28; published 2008 August 21

ABSTRACT

We present the first resolved images of the eclipsing binary β Lyrae, obtained with the CHARA Array interferometer and the MIRC combiner in the H band. The images clearly show the mass donor and the thick disk surrounding the mass gainer at all six epochs of observation. The donor is brighter and generally appears elongated in the images, the first direct detection of photospheric tidal distortion due to Roche lobe filling. We also confirm expectations that the disk component is more elongated than the donor and is relatively fainter at this wavelength. Image analysis and model fitting for each epoch were used for calculating the first astrometric orbital solution for β Lyrae, yielding precise values for the orbital inclination and position angle. The derived semimajor axis also allows us to estimate the distance of β Lyrae; however, systematic differences between the models and the images limit the accuracy of our distance estimate to about 15%. To address these issues, we will need a more physical, self-consistent model to account for all epochs as well as the multiwavelength information from the eclipsing light curves.

Subject headings: binaries: eclipsing — infrared: stars — stars: fundamental parameters — stars: individual (β Lyrae) — techniques: interferometric

1. INTRODUCTION

Interacting binaries are unique testbeds for many important astrophysical processes, such as mass and momentum transfer, accretion, tidal interaction, etc. These processes provide information on the evolution and properties of many types of objects, including low-mass black holes and neutron stars (in low-mass X-ray binaries), symbiotic binaries, cataclysmic variables, novae, etc. Although these types of objects are widely studied by indirect methods such as spectroscopy, radial velocity (RV), and sometimes eclipse mapping, very few of them have been directly resolved because they are very close to each other and far away from us. Thus, directly imaging interacting binaries, although very challenging, will greatly help us to improve our understanding of these objects.

The star β Lyrae (Sheliak, HD 174638, HR 7106; $V = 3.52, H = 3.35$) is a well-known interacting and eclipsing binary that has been widely studied since its discovery in 1784 (Goodricke 1785). According to the current picture (Harmanec 2002), the system consists of a B6–B8 II Roche lobe filling mass-losing star, which is generally denoted as the donor or the primary, and an early B-type mass-gaining star, which is generally denoted as the gainer or the secondary. The donor, which was initially more massive than the gainer, has a current mass of about 3 $M_\odot$, while the gainer has a mass of about 13 $M_\odot$. It is thought that the gainer is completely embedded in a thick accretion disk with bipolar jetlike structures perpendicular to the disk, which creates a light-scattering halo above its poles (Wilson 1974; Harmanec 2002, and references therein). The orbit of the system is highly circular (Harmanec & Scholz 1993) and is very close to edge-on (Linnell 2000). Recent RV study on the ephemeris of the system gives a period of 12.94 days (Ak et al. 2007). The period is increasing at a rate of ~19 s yr^{-1} due to the high mass transfer rate, $2 \times 10^{-5}\ M_\odot\ \mathrm{yr}^{-1}$, of the system.

The primary eclipse of the light curve (i.e., at phase 0) corresponds to the eclipse of the donor. In the *UBV* bands, the surface of the donor is brighter than that of the gainer, and therefore the primary minimum is deeper than the secondary minimum. At longer wavelengths, however, the studies of Jameson & Longmore (1976) and Zeilik et al. (1982) suggest that the relative depth of the secondary minimum in the light curve gradually deepens and becomes deeper than the primary minimum at wavelengths longer than 3.6 μm.

Light-curve studies and theoretical models have shown that, at the distance of 296 pc (van Leeuwen 2007), the estimated separation of the binary is only 0.92 milliarcseconds (mas; 58.5 $R_\odot$). The angular diameter of the donor is ~0.46 mas (29.4 $M_\odot$), and the disk surrounding the gainer is only ~1 mas across (e.g., Linnell 2000; Harmanec 2002). The goal of directly imaging β Lyr, therefore, requires the angular resolution only achievable by today's long-baseline interferometers. Recently, Schmitt et al. (2008) used the NPOI interferometer to image successfully the Hα emission of β Lyr, an update to the pioneering work of Harmanec et al. (1996). Also, radio work using MERLIN found a nebula surrounding the secondary but could not resolve its bipolar shape (Umana et al. 2000). Despite recent progress, the individual objects of the system have not been resolved yet, putting even a simple astrometric orbit beyond our reach.

In this study, we present the first resolved images of the β Lyr system at multiple phases, obtained with the CHARA Array and the MIRC combiner. We give a brief introduction to our observations and data reduction in § 2. We present our aperture synthesis images with simple models in § 3. In § 4 we discuss our astrometric orbit of β Lyr, and we give the outlook for future work in § 5.

2. OBSERVATIONS AND DATA REDUCTION

Our observations were conducted at the Georgia State University (GSU) Center for High Angular Resolution Astronomy (CHARA) interferometer array along with the MIRC instrument. The CHARA array, located on Mount Wilson and consisting of six 1 m telescopes, is the longest optical/IR interferometer array in the world (ten Brummelaar et al. 2005). It has 15 baselines ranging from 34 to 331 m, providing resolutions up to ~0.5 mas at H band and ~0.7 mas at K band.

[1] University of Michigan Astronomy Department, 941 Dennison Building, Ann Arbor, MI 48109-1090; mingzhao@umich.edu.
[2] The CHARA Array, Georgia State University.
[3] University of St. Andrews, Scotland, UK.
[4] University of Cambridge, UK.
[5] National Optical Astronomy Observatory, NOAO, Tucson, AZ.

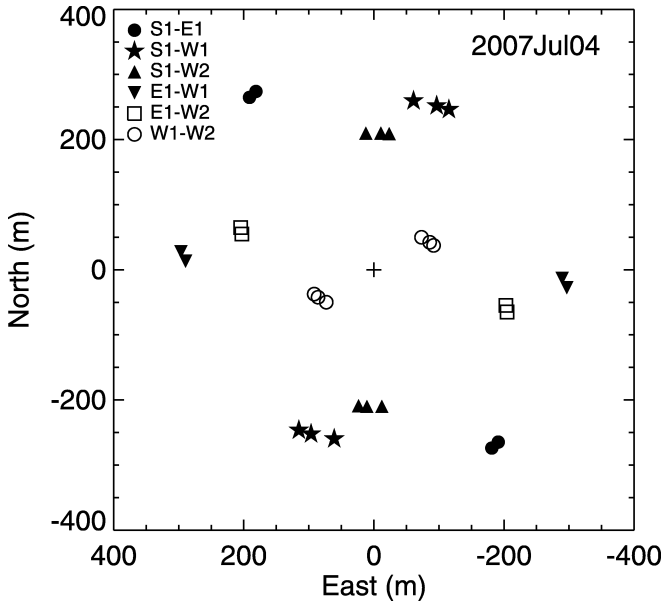

FIG. 1.—Telescope spatial coverage of β Lyr on UT 2007 July 4, using the W1-W2-S1-E1 configuration of CHARA. The symbols stand for different baselines. The longest projected baseline in this observation is 328.5 m, corresponding to a resolution of 0.52 mas in the H band. The actual UV coverage is similar to this spatial coverage, but each point spreads over eight wavelength channels.

The Michigan Infra-Red Combiner (MIRC) was used here to combine four CHARA telescopes together for true interferometric imaging in H band, providing six visibilities, four closure phases, and four triple amplitudes simultaneously in eight narrow spectral bands (Monnier et al. 2004, 2006). Specifically, the β Lyr system was observed on six nights in 2006 and 2007 using array configurations optimized for good imaging (equal Fourier coverage in all directions) and following standard observing procedures (M. Zhao et al. 2008, in preparation; Monnier et al. 2007). A typical baseline coverage of our observations is shown in Figure 1. In short, we observed our target along with two or three calibrators on each night; a complete observing log is listed in Table 1.

The data reduction process follows the pipeline outlined by Monnier et al. (2007). In brief, after frame co-adding, background subtraction, and Fourier transform of the raw data, fringe amplitudes and phases are used to form squared visibilities and triple products. Photometric calibrations are estimated using shutter matrix measurements and partial beam chopping. Finally, calibrators with known sizes (see Table 1) are used to calibrate the drifts in overall system response before obtaining final calibrated squared visibilites and complex triple amplitudes.

TABLE 1

OBSERVATION LOGS FOR β LYR

Date (UT)	Mean MJD	Telescopes	N_{blk}[a]	Calibrators[b]
2006 Oct 16	54,024.17	W1-W2-S2-E2	1	29 Peg, υ And
2007 Jul 3	54,284.25	W1-W2-S1-E1	3	γ Lyr, υ Peg, υ And
2007 Jul 4	54,285.26	W1-W2-S1-E1	3	γ Lyr, υ Peg, υ And
2007 Jul 7	54,288.22	W1-W2-S1-E1	3	γ Lyr, υ Peg, σ Cyg
2007 Jul 9	54,290.25	W1-W2-S1-E1	3	γ Lyr, υ Peg
2007 Jul 12	54,293.26	W1-W2-S1-E1	3	γ Lyr, σ Cyg

[a] N_{blk} = number of data blocks

[b] Calibrator diameters (mas): 29 Peg = 1.017 ± 0.027, υ And = 1.098 ± 0.007, σ Cyg = 0.542 ± 0.021 (A. Merand 2008, private communication); γ Lyr = 0.74 ± 0.10 (Leggett et al. 1986); υ Peg = 1.01 ± 0.04 (Blackwell & Lynas-Gray 1994).

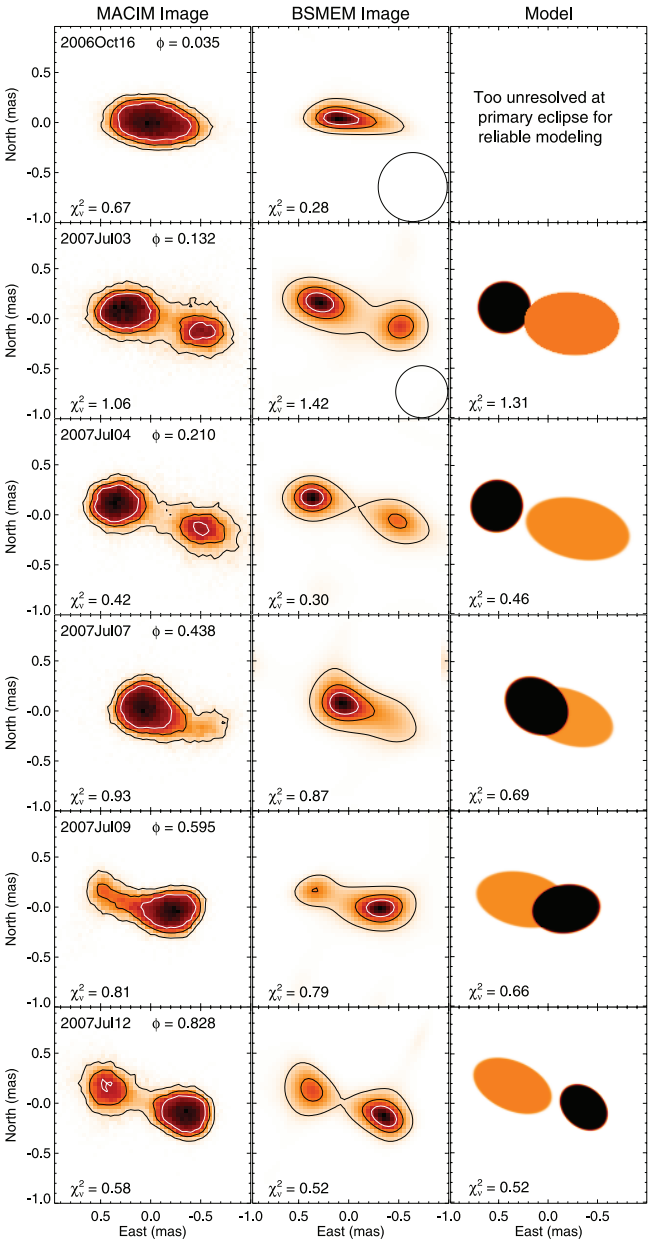

FIG. 2.—Reconstructed images and two-component models of β Lyr. The left, middle, and right columns show the MACIM, BSMEM, and model images, respectively. Darker colors indicate higher intensity. The darker component is the donor. The contours in the images correspond to 0.3, 0.6, and 0.9 of the peak intensity. Observing dates and corresponding phases (from the ephemeris in Ak et al. 2007) are labeled in the first column. The best-fit χ^2/dof of each image is labeled in the bottom left corner. The resolution of the reconstructed images is 0.69 mas for the first epoch and 0.52 mas for the other five epochs, and the corresponding beams are shown in the first and second epochs in the middle panels, respectively. Due to lack of enough resolution and the complexity of the radiative transfer at the first epoch when the star is behind the disk, no reliable model is available for our limited data.

3. SYNTHESIS IMAGING AND MODELING

For imaging with optical interferometry data, we employed two independent applications: Markov-Chain Imager for Optical Interferometry (MACIM) (Ireland et al. 2006) and the maximum-entropy–based BSMEM (Buscher 1994). Further description and a detailed comparison of these algorithms on simulated data appear in Lawson et al. (2004, 2006). Both of these algorithms benefit from use of prior information, gen-

TABLE 2
ORBITAL POSITIONS OF β LYR

		MACIM		BSMEM		MODEL		
DATE	PHASE	Sep. (mas)	P.A. (deg)	Sep. (mas)	P.A. (deg)	Sep. (mas)	P.A. (deg)	Flux Ratio (Donor/Gainer)
2007 Jul 3	0.132	0.811	255.4	0.853	253.7	0.701 ± 0.091	256.3 ± 4.0	1.01 ± 0.11
2007 Jul 4	0.210	0.891	253.3	0.886	254.4	0.852 ± 0.045	254.2 ± 2.1	$1.16^{+0.20}_{-0.15}$
2007 Jul 7	0.438	...	...	...	...	0.338 ± 0.105	250.8 ± 7.3	3.51 ± 1.27
2007 Jul 9	0.595	...	...	0.675	73.9	0.454 ± 0.042	77.9 ± 1.4	2.43 ± 0.28
2007 Jul 12	0.828	0.842	72.3	0.783	69.6	0.754 ± 0.063	73.2 ± 0.8	$1.32^{+0.67}_{-0.27}$

NOTE.—Sep. = separation. Some positions are omitted for images whose centroids cannot be separated.

erally based on lower resolution data. For β Lyr we began each image reconstruction with a two-component Gaussian model that mainly acts to limit the field of view of the image. The final images do not resemble the priors except in general extent; i.e., the final positions, relative sizes, and relative brightnesses are not dependent on the priors. The final reconstructed images from both methods are shown in Figure 2. The MACIM and BSMEM images are consistent with each other, although they use very different algorithms, giving confidence to the image fidelity. Any differences, such as the more Gaussian shapes for BSMEM compared to the more "flat-top" profiles for MACIM, illustrate the limitations of our data set. We present here results from both algorithms in lieu of image "error bars" that are notoriously difficult to define in aperture synthesis imaging.

The six epochs span all phases of the orbit, changing from middle primary eclipse (phase = 0.035) to nearly maximum elongation (phase = 0.210 and 0.828) and secondary eclipse (phase = 0.438). The system is well resolved into two separate components at phases close to the maximum elongation. Since the primary eclipse is still the deeper one in the *H* band (Jameson & Longmore 1976), we can conclude that the object with higher surface brightness is the mass donor star (i.e., the component moving from left to right in the 2007 July sequence). The donor is partially resolved and appears elongated at all epochs except at phase 0.035, when it is blocked by the disk, directly confirming its Roche lobe filling picture. The thick disk surrounding the gainer is also resolved and appears elongated. At the first epoch (phase = 0.035), we see mostly the emission from the disk superposed with a small amount of light from the poles of the donor.

We can extract further information by constructing a simple two-component model to determine the separation and position angle for each epoch. We assume that the donor and gainer can be modeled as uniform ellipses. Other models, such as two truncated Gaussian ellipses, a raindrop-shaped Roche lobe filling star with a truncated Gaussian disk, etc., were also considered and gave equivalent results due to limited resolution. Therefore, for simplicity and to minimize the degrees of freedom of the model, uniform ellipses are adopted. The free parameters in the models are the semimajor and semiminor axes of the two components, their individual position angles, the separation and position angle of the system, and the flux ratio of the donor and the disk. We used ephemeris data from Ak et al. (2007) to fix which component was in front during modeling. Due to degeneracies in the separation and the dimensions of the blocked component when the two are overlapping with each other, the size of the blocked component is fixed to the average from the two separated epochs, 2007 July 4 and 2007 July 12. The best-fit models for all epochs are presented in the third column of Figure 2, and the resulting positions and total flux ratios from the models are listed in Table 2, along with the results obtained from the image centroids where separating the two components is possible. Errors of the positions are estimated from the χ^2 surfaces of each parameter where $\Delta\chi^2 = 1$ or from the scatter in fits within each night, whichever is larger.

The models confirm that the smaller and more circular component, i.e., the donor, has higher surface brightness and total flux than the more elongated disk around the gainer. The ellipse size of the donor from the models, when averaged over all the epochs, is 0.62 ± 0.16 mas along the major axis and 0.52 ± 0.14 mas along the minor axis, which confirms the images that the donor is elongated but slightly larger than that from the theoretical models (Harmanec 2002). The averaged size of the disk surrounding the gainer is 1.04 ± 0.11 mas along the major axis, consistent with the size of the images of the first epoch as well as theoretical models (Harmanec 2002) and the Hα disk of Schmitt et al. (2008). The minor axis of the disk is 0.63 ± 0.07 mas, larger than that expected in theoretical models (Bisikalo et al. 2000; Linnell 2000), implying that this extended structure is perhaps from the electron scattering and/or free-free emission from the halo above the poles of the gainer (Jameson & Longmore 1976; Zeilik et al. 1982).

We also compared the flux ratios from our models with those obtained from *H*-band light curves. The light curves from literatures[6] give a value of $(f_1 + f_2)/f_p = 1.86$, where f_1, f_2, and f_p are the fluxes of the donor, the disk of the gainer, and the flux at the primary eclipse. Because the donor is not completely eclipsed by the disk at primary eclipse (Linnell 2000), $f_p = f_2 + af_1$, where a is the fraction of the donor flux that goes through. Therefore, we can infer that $f_1/f_2 > 0.86$, consistent with our flux ratios derived from the models at phase 0.210 and 0.828, i.e., 1.16 and 1.32. In addition, taking the average

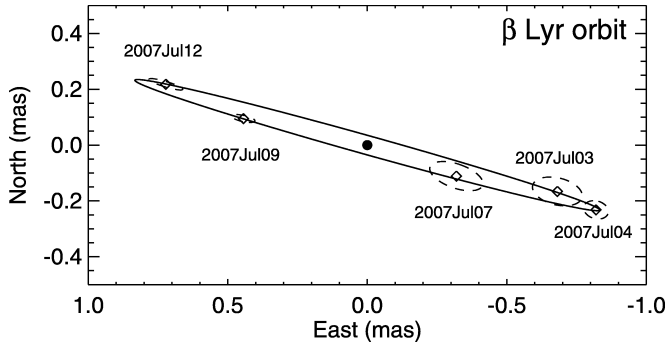

FIG. 3.—The best-fit relative orbit of β Lyr (*solid line*). The donor is indicated as a filled dot in the center. Positions of each epoch are shown by the open dots, surrounded by their error ellipses in dashed lines. The upper part of the orbit is located toward the observer.

[6] The light curve of Zeilik et al. (1982) at the *H* band gives a −0.61 mag difference between the total magnitude of the system and the magnitude at primary eclipse. Interpolating the *J*- and *K*-band light curves of Jameson & Longmore (1976), we can obtain an *H*-band magnitude difference of −0.74. Taking the average of the two, we get a difference of 0.675 mag, corresponding to a $(f_1 + f_2)/f_p$ value of 1.86.

TABLE 3
PARAMETERS OF β LYR

	MACIM	BSMEM	Model
Inclination (deg)	92.10 ± 1.24	91.96 ± 1.65	92.25 ± 0.82
Ω (deg)	253.22 ± 1.97	251.87 ± 1.83	254.39 ± 0.83
Semimajor axis (mas)	0.976 ± 0.083	0.993 ± 0.122	0.865 ± 0.048
Distance (pc)	276 ± 23	271 ± 33	312 ± 17

of the two values, $f_1/f_2 = 1.24$, we get $a = 0.165$, suggesting that 16.5% of flux from the donor goes through at the primary eclipse. This also implies that the donor contributes ~17% of total flux at the primary eclipses, consistent with the 20% value of Linnell (2000).

The goodness-of-fit values of the models (i.e., χ^2/dof, included in each panel of Fig. 2) are in general similar to those of the images. Nevertheless, discrepancies exist between the models and the images. For instance, the components' separations from the models are slightly smaller than the images. The gainer disk appears bigger in the models than in the images. These properties demonstrate the complexity of β Lyr and suggest that the disk may be asymmetric. They also highlight the deficiencies in our models and underscore the need for a self-consistent model that treats the radiative transfer properly and accounts for all epochs simultaneously.

4. THE ORBIT OF β LYR

Despite the deficiencies in our simplified models, the positions of each component's center of light are well constrained, especially near the maximum elongation of the orbit. Thus, the above results, along with the elements obtained from RV and light-curve studies, allow us to calculate the astrometric orbit of β Lyr for the first time. We adopt $P = 12.9414$ days and $T_{\rm mini} =$ JD 2,454,283.0430 (on 2007 July 1) from the recent ephemeris[7] (Ak et al. 2007) and $e = 0$ (Harmanec 2002). The best-fit orbit using the model positions is shown in Figure 3. The resultant inclination, position angle of the ascending node (Ω), and semimajor axis are listed in Table 3. Other orbital solutions using positions from the images are also listed in the table. Errors of orbital elements are estimated using Monte Carlo simulations. The three sets of inclination and Ω in Table 3 are consistent with each other and suggest a retrograde orbit (i.e., position angle decreasing with time). Our estimate on Ω is roughly consistent with the 248.8° value in Schmitt et al. (2008) and is almost perpendicular to the orientation of the jet (163.5°) implied by Hoffman et al. (1998).

[7] $T_{\rm mini}$ (phase 0) is the epoch of primary minimum light.

We can also estimate the distance of β Lyr using orbital parallax (see Table 3) by combining its angular semimajor axis with the linear $a \sin i$ value, $57.87 \pm 0.62\ M_\odot$.[8] The distance from our models, 314 ± 17 pc, is larger than that from the images, 278 ± 24 pc and 274 ± 34 pc, but they are all consistent within errors with the *Hipparcos* distance, 296 ± 16 pc (van Leeuwen 2007). Finally, using the newly estimated $M \sin^3 i$ for both components (see footnote 8) together with the inclination from the models, we get mass of the gainer, $12.76 \pm 0.27\ M_\odot$, and mass of the donor, $2.83 \pm 0.18\ M_\odot$.

5. FUTURE WORK

We have presented only simple two-component models in this work since we mostly focus on the orbital positions of β Lyr. We have already discussed problematic discrepancies between the models and the images and also some internal inconsistencies between the model epochs. The systematic difference in component separations between the images compared to the model fits poses the most severe problem, limiting the accuracy of our distance estimates to ~15%. To address these issues and better understand other physical properties of β Lyrae, a more physical, self-consistent model is required that treats the radiative transfer and the sizes of the two components properly, accounts for all epochs simultaneously, and incorporates the multiwavelength information from eclipsing light curves.

We thank Michael Ireland for the MACIM package used in this work. We also thank the referees for valuable suggestions and comments. The CHARA Array is funded by the National Science Foundation through NSF grants AST-0307562 and AST-0606958 and by the Georgia State University. We thank the support for this work by the Michelson Graduate Fellowship (M. Z.), the NSF grants AST-0606861 (D. G.), NSF-AST 0352723, NSF-AST 0707927, NASA NNG 04GI33G (J. D. M.), and EU grant MOIF-CT-2004-002990 (N. T.). E. P. was formally supported by the Michelson Postdoctoral Fellowship and is currently supported by a Scottish Universities Physics Association (SUPA) advanced fellowship.

Facility: CHARA

[8] We obtain the semimajor axis by combining the semiamplitude of the gainer K_1 (41.4 ± 1.3 km s^{-1}, Harmanec & Scholz 1993; 42.1 ± 1.3 km s^{-1} [error assumed], Bisikalo et al. 2000; 35.4 ± 2.7 km s^{-1} [from their Fig. 5], Ak et al. 2007; yielding a weighted average of 41.1 ± 2.7 km s^{-1}) with that for the donor K_2 (185.27 ± 0.20 km s^{-1}, Ak et al. 2007). We derive $q = M_2/M_1 = 0.222 \pm 0.013$, $a \sin i = 57.87 \pm 0.62\ M_\odot$, $M_1 \sin^3 i = 12.73 \pm 0.27\ M_\odot$, and $M_2 \sin^3 i = 2.82 \pm 0.18\ M_\odot$

REFERENCES

Ak, H., et al. 2007, A&A, 463, 233
Bisikalo, D. V., Harmanec, P., Boyarchuk, A. A., Kuznetsov, O. A., & Hadrava, P. 2000, A&A, 353, 1009
Blackwell, D. E., & Lynas-Gray, A. E. 1994, A&A, 282, 899
Buscher, D. F. 1994, Proc. SPIE, 2200, 260
Goodricke, J. 1785, Phil. Trans. Roy. Soc. 75
Harmanec, P. 2002, Astron. Nachr., 323, 87
Harmanec, P., & Scholz, G. 1993, A&A, 279, 131
Harmanec, P., et al. 1996, A&A, 312, 879
Hoffman, J. L., Nordsieck, K. H., & Fox, G. K. 1998, AJ, 115, 1576
Ireland, M. J., Monnier, J. D., & Thureau, N. 2006, Proc. SPIE, 6268E, 62681T
Jameson, R. F., & Longmore, A. J. 1976, MNRAS, 174, 217
Lawson, P. R., et al. 2004, Proc. SPIE, 5491, 886
———. 2006, Proc. SPIE, 6268E, 62681U
Leggett, S. K., Mountain, C. M., Selby, M. J., Blackwell, D. E., Booth, A. J., Haddock, D. J., & Petford, A. D. 1986, A&A, 159, 217
Linnell, A. P. 2000, MNRAS, 319, 255
Monnier, J. D., Berger, J.-P., Millan-Gabet, R., & Ten Brummelaar, T. A. 2004, Proc. SPIE, 5491, 1370
Monnier, J. D., et al. 2006, Proc. SPIE, 6268, 62681P
———. 2007, Science, 317, 342
Schmitt, H. R., et al. 2008, ApJ, submitted (arXiv:0801.4772)
ten Brummelaar, T. A., et al. 2005, ApJ, 628, 453
Umana, G., Maxted, P. F. L., Trigilio, C., Fender, R. P., Leone, F., & Yerli, S. K. 2000, A&A, 358, 229
van Leeuwen, F. 2007, Hipparcos, the New Reduction of the Raw Data (Astrophys. Space Sci. Library 350; Dordrecht: Springer)
Wilson, R. E. 1974, ApJ, 189, 319
Zeilik, M., Heckert, P., Henson, G., & Smith, P. 1982, AJ, 87, 1304